Fast polarization-state tracking scheme based on radius-directed linear Kalman filter

Yanfu Yang,[1,*] Guoliang Cao,[1] Kangping Zhong,[2] Xian Zhou,[2] Yong Yao,[1] Alan Pak Tao Lau,[2] and Chao Lu[3]

[1] *Department of Electronic and Information Engineering, Shenzhen Graduate School, Harbin Institute of Technology, ShenZhen, GuangDong, China*

[2] *Photonics Research Center, Department of Electrical Engineering, The Hong Kong Polytechnic University, Hung Hom, Kowloon, Hong Kong, China*

[3] *Photonics Research Center, Department of Electronic and Information Engineering, The Hong Kong Polytechnic University, Hung Hom, Kowloon, Hong Kong, China*

[*] *yangyanfu@hotmail.com*

Abstract: We propose and experimentally demonstrate a fast polarization tracking scheme based on radius-directed linear Kalman filter. It has the advantages of fast convergence and is inherently insensitive to phase noise and frequency offset effects. The scheme is experimentally compared to conventional polarization tracking methods on the polarization rotation angular frequency. The results show that better tracking capability with more than one order of magnitude improvement is obtained in the cases of polarization multiplexed QPSK and 16QAM signals. The influences of the filter tuning parameters on tracking performance are also investigated in detail.

OCIS codes: (060.1660) Coherent communications; (120.3930) Metrological instrumentation.

References and links

1. P. M. Krummrich and K. Kotten, "Extremely fast (microsecond timescale) polarization changes in high speed long haul WDM transmission systems," in *Optical Fiber Communication Conference*, 2004 OSA Technical Digest Series (Optical Society of America, 2004), paper FI3.
2. V. B. Ribeiro, J. C. Oliveira, J. C. Diniz, E. Rosa, R. Silva, E. P. Silva, L. H. Carvalho, and A. C. Bordonalli, "Enhanced Digital Polarization Demultiplexation via CMA Step Size Adaptation for PM-QPSK Coherent Receivers," in *Optical Fiber Communication Conference*, OSA Technical Digest (Optical Society of America, 2012), paper OW3H.4.
3. I. Fatadin, D. Ives, and S. J. Savory, "Blind equalization and carrier phase recovery in a 16-QAM optical coherent system," J. Lightwave Technol. **27**(15), 3042–3049 (2009).
4. B. Szafraniec, B. Nebendahl, and T. Marshall, "Polarization demultiplexing in Stokes space," Opt. Express **18**(17), 17928–17939 (2010).
5. P. Johannisson, H. Wymeersch, M. Sjödin, A. S. Tan, E. Agrell, P. A. Andrekson, and M. Karlsson, "Convergence comparison of the CMA and ICA for blind polarization demultiplexing," J. Opt. Commun. Netw. **3**(6), 493–501 (2011).
6. B. Szafraniec, T. S. Marshall, and B. Nebendahl, "Performance monitoring and measurement techniques for coherent optical systems," J. Lightwave Technol. **31**(4), 648–663 (2013).
7. N. J. Muga and A. N. Pinto, "Adaptive 3-D Stokes Space-Based Polarization Demultiplexing Algorithm," J. Lightwave Technol. **32**(19), 3290–3298 (2014).
8. T. Marshall, B. Szafraniec, and B. Nebendahl, "Kalman filter carrier and polarization-state tracking," Opt. Lett. **35**(13), 2203–2205 (2010).
9. S. Zhang, P. Y. Kam, C. Yu, and J. Chen, "Frequency Offset Estimation Using Kalman Filter in Coherent Optical Phase-Shift Keying Systems," in *Conference on Lasers and Electro-Optics 2010,* OSA Technical Digest (Optical Society of America, 2010), paper CThDD4.
10. T. Inoue and S. Namiki, "Carrier recovery for M-QAM signals based on a block estimation process with Kalman filter," Opt. Express **22**(13), 15376–15387 (2014).
11. L. Pakala and B. Schmauss, "Joint compensation of phase and amplitude noise using extended Kalman filter in coherent QAM systems," in *European Conference on Optical Communication* (IEEE, 2014), paper Tu.1.3.2.
12. G. Cao, Y. Yang, K. Zhong, X. Zhou, Y. Yao, A. P. T. Lau, and C. Lu, "Fast Polarization-State Tracking Based on Radius-Directed Linear Kalman Filter," in *Optical Fiber Communication Conference*, 2015 OSA Technical Digest Series (Optical Society of America, 2015), paper Th4F.2.

#236586 Received 22 Apr 2015; revised 16 Jul 2015; accepted 17 Jul 2015; published 22 Jul 2015

13. G. Welch and G. Bishop, "An introduction to the Kalman filter," in *Proceedings of the Siggraph Course*, Los Angeles (2001).
14. S. J. Savory, "Digital filters for coherent optical receivers," Opt. Express **16**(2), 804–817 (2008).

1. Introduction

Advanced modulation formats, polarization division multiplexing (PDM), coherent detection and digital signal processing (DSP) are the main enabling technologies for achieving high spectral efficiency in next-generation 400Gb/s and 1Tb/s fiber optic communication systems. In PDM-based long-haul fiber communication systems, polarization-state tracking and demultiplexing is one of the key DSP modules in the coherent receiver side. Different from chromatic dispersion which is a static impairment, polarization-state along the fiber is random in nature and can fluctuate quickly under external vibration and with time. The experiment have shown that Stokes vector movements in coiled patch fiber cables and spooled dispersion compensating fiber (DCF) can be as large as 45000 rotations/sec under mechanical vibrations [1]. Conventional blind polarization de-multiplexing algorithms including constant modulus algorithm (CMA), multi-modulus algorithm (MMA) and their variants have the disadvantages of low convergence/tracking speed and singularity problem [2,3]. Therefore, several alternative polarization demultiplexing algorithms including Stokes space (SS), independent component analysis (ICA), and extended Kalman filter (EKF) are proposed to solve the problems above. Among these algorithms, SS scheme can account for the relative phase offset between the two polarizations before de-multiplexing and can also achieve convergence performance after less than 100 sampled points with better performance than CMA/MMA, the gradient optimization ICA and EKF algorithms [2–6]. However, the SS scheme with plane fitting [6] has degraded performance under time-varying state of polarization, which can be improved by an adaptive SS algorithm [7]. Recently, Kalman filter has attracted attention for its application potentials in polarization/phase tracking [8], frequency offset estimation [9,10], and nonlinear phase noise mitigation [11]. However, the EKF-based polarization/phase simultaneous tracking scheme imposes stringent requirement on frequency offset estimation accuracy before de-multiplexing, which will limit its possible application scenarios [8]. Recently, we proposed a fast polarization tracking scheme based on radius-directed linear Kalman filter (RD-LKF) [12], which is immune to frequency offset and has fast convergence and tracking performance.

This paper extends the work in [12] and experimentally demonstrated the capability of the RD-LKF scheme on tracking fast polarization-state for both polarization multiplexed quadrature phase-shift keying (QPSK) and 16 quadrature amplitude modulation (16QAM). The operating principle of RD-LKF is proposed and the influence of the filter tuning parameters on tracking performance is analyzed in detail. The experimental results show that the RD-LKF has similar converges speed with SS and can track polarization rotation an order of magnitude faster than the CMA/MMA algorithm for QPSK and 16QAM signals, respectively. Compared with the previous EKF method, our scheme is immune to carrier phase noise and frequency offset and is easy to implement due to reduced computation complexity.

2. Principle

2.1 RD-LKF for QPSK

The received signal of a typical optical transmission system can be expressed as follow [12]:

$$\boldsymbol{Z}(t) = \alpha \boldsymbol{J}(t)\boldsymbol{X}(t)e^{j(\Delta\omega t)}e^{j\theta(t)} + \boldsymbol{\xi}(t), \tag{1}$$

in which $\boldsymbol{X}(t)$, $\boldsymbol{Z}(t)$, $\Delta\omega$, $\boldsymbol{J}(t)$, $\theta(t)$, α, $\boldsymbol{\xi}(t)$ represent the transmitted signal, the received signal in dual-polarization, the frequency offset between the laser source and the local oscillator, the time-varying Jones matrix caused by random birefringence in fiber, carrier phase noise, loss

#236586 Received 22 Apr 2015; revised 16 Jul 2015; accepted 17 Jul 2015; published 22 Jul 2015

factor and additive white Gaussian noise in dual-polarization, respectively. The polarization demultiplexing process can be expressed as:

$$\boldsymbol{X}(t)\cdot e^{j(\Delta\omega t)}\cdot e^{j\theta(t)}+\boldsymbol{\xi}'(\mathrm{t})=(\alpha\boldsymbol{J}(t))^{-1}\boldsymbol{Z}(t)=\begin{bmatrix} a(t)+jb(t) & c(t)+jd(t) \\ -c(t)+jd(t) & a(t)-jb(t)\end{bmatrix}\begin{bmatrix} Z_x(t) \\ Z_y(t)\end{bmatrix}, \quad (2)$$

in which the inverse of the slowly varying Jones matrix $\boldsymbol{J}(t)$ is expressed by four real-valued parameters a, b, c, d, which means that this scheme is immune to the singularity problem [6].

After applying the above model to linear Kalman filter and using time discretization with $t = kT_s$ (T_s is the symbol period), the following relationship is obtained, where j = sqrt(−1):

$$\boldsymbol{H}(k)=\begin{bmatrix} Z_x(k) & jZ_x(k) & Z_y(k) & jZ_y(k) \\ Z_y(k)-jZ_y(k) & -Z_x(k) & jZ_x(k)\end{bmatrix}, \quad (3)$$

$$\boldsymbol{S}(k)=[a(k)\,b(k)\,c(k)\,d(k)]^T, \quad (4)$$

$$\boldsymbol{U}(k)=\boldsymbol{H}(k)\boldsymbol{S}(k)+\boldsymbol{v}(k), \quad (5)$$

$$\boldsymbol{S}(k)=\boldsymbol{S}(k-1)+\boldsymbol{w}(k). \quad (6)$$

The $\boldsymbol{U}(k)$ represents the polarization demultiplexed signal. Equations (5) and (6) are the measurement equation and process equation, where $\boldsymbol{v}(k)$, $\boldsymbol{w}(k)$ are the measurement noise and process noise, respectively [13]. The RD-LKF scheme is inherently linear and has reduced dimension $\boldsymbol{S}(k)$ and $\boldsymbol{H}(k)$ as a result of no phase estimation involved compared to EKF. The filtering process is shown as Fig. 1, in which $\boldsymbol{P}^-(k)$, $\boldsymbol{P}(k)$, $\Delta\boldsymbol{U}(k)$ and $\boldsymbol{K}(k)$ are called priori estimate error covariance, posteriori estimate error covariance, residual and Kalman gain [13]. The Kalman prediction Eqs. (7) and (8) and the Kalman update Eqs. (9)-(12) are presented in the below. The state vector $\boldsymbol{S}(k)$ is estimated by making the measurement prediction $\boldsymbol{U}(k)$ locked to ideal circles formed by the rotation of constellations. No decision is required for QPSK and three-level decisions are required for 16QAM to compute $\Delta\boldsymbol{U}(k)$. Obviously the RD-LKF has relatively complex equations compared to CMA/MMA. As a variant of Kalman filter, the RD-LKF inherently converges faster than CMA/MMA via the intelligent gain coefficient $\boldsymbol{K}$, which is also updated by taking into account the priori and posteriori estimate error covariance.

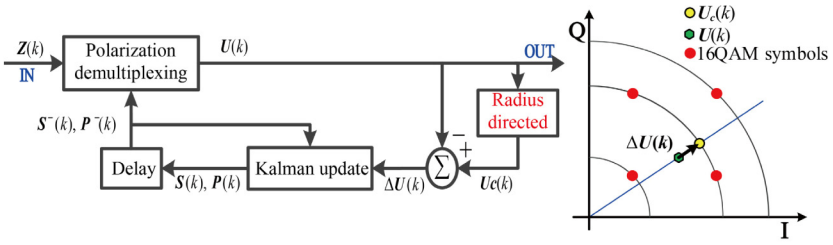

Fig. 1. Kalman process and the computation of $\Delta\boldsymbol{U}(k)$.

$$\boldsymbol{S}^-(k)=\boldsymbol{S}(k-1) \quad (7)$$

$$\boldsymbol{P}^-(k)=\boldsymbol{P}(k-1)+\boldsymbol{Q} \quad (8)$$

$$\boldsymbol{K}(k)=\boldsymbol{P}^-(k)\boldsymbol{H}^{\mathrm{T}}(k)(\boldsymbol{H}(k)\boldsymbol{P}^-(k)\boldsymbol{H}^{\mathrm{T}}(k)+\boldsymbol{R})^{-1} \quad (9)$$

$$\Delta\boldsymbol{U}(k)=\boldsymbol{U}_c(k)-\boldsymbol{U}(k)=\boldsymbol{U}_c(k)-\boldsymbol{H}(k)\boldsymbol{S}^-(k) \quad (10)$$

#236586 Received 22 Apr 2015; revised 16 Jul 2015; accepted 17 Jul 2015; published 22 Jul 2015

$$\boldsymbol{S}(k) = \boldsymbol{S}^{-}(k) + \boldsymbol{K}(k)\Delta\boldsymbol{U}(k) \tag{11}$$

$$\boldsymbol{P}(k) = \boldsymbol{P}^{-}(k) - \boldsymbol{K}(k)\boldsymbol{H}(k)\boldsymbol{P}^{-}(k) \tag{12}$$

In each iteration, the measurement prediction $\boldsymbol{U}(k)$ is first calculated from the state prediction $\boldsymbol{S}^{-}(k)$ and input $\boldsymbol{Z}(k)$. Then, the so called actual measurement $\boldsymbol{U}_c(k)$ is obtained by finding a nearest constellations circle apart from $\boldsymbol{U}(k)$. $\boldsymbol{U}_c(k)$ is the vector which has the same phase with $\boldsymbol{U}(k)$ and locates on the nearest circle as shown in Fig. 1, and can be calculated by the following expression:

$$\boldsymbol{U}_c(k) = \left[\frac{r_x \bullet U_x(k)}{|U_x(k)|} \quad \frac{r_y \bullet U_y(k)}{|U_y(k)|} \right]^T, \tag{13}$$

in which $U_{x,y}$ is two polarization components of $\boldsymbol{U}(k)$, $r_{x,y}$ is the radius of the nearest circles for $U_{x,y}$. In QPSK format, $r_{x,y}$ can be set to sqrt(P_{ave}), in which P_{ave} is the average power in each polarization. For a determinate measurement prediction, the corresponding residual can be calculated as $\Delta\boldsymbol{U}(k) = \boldsymbol{U}_c(k) - \boldsymbol{U}(k)$. In our proposed radius-directed Kalman filter the residual is immune to frequency offset and phase noise since $\boldsymbol{U}_c(k)$ has the same phase as $\boldsymbol{U}(k)$. In the above filter, $\boldsymbol{Q}$ and $\boldsymbol{R}$ describe the process noise covariance and measurement noise covariance which are further treated as two important filter tuning parameters. In this work, $\boldsymbol{Q}$ and $\boldsymbol{R}$ can be considered as scaled identities.

2.2 RD-LKF for 16QAM

If the above scheme is directly employed for 16QAM format signal with $r_{x,y}$ = {sqrt(P_{ave}/5), sqrt(P_{ave}), sqrt(9P_{ave}/5)}, it may occasionally has slow convergence. An elegant method to deal with this problem is to employ double measurement method (DME), as suggested by B. Szafraniec [6]. The resultant $\boldsymbol{H}_{DME}$ and $\Delta\boldsymbol{U}_{DME}$ can be substituted into Eqs. (14)-(16) with the following expressions:

$$\boldsymbol{H}_{DME}(k) = \begin{bmatrix} \boldsymbol{H}(k) \\ \boldsymbol{H}(k) \end{bmatrix} \tag{14}$$

$$\boldsymbol{U}_{DME}(k) = \begin{bmatrix} \boldsymbol{U}(k) \\ \boldsymbol{U}(k) \end{bmatrix} = \boldsymbol{H}_{DME}(k)\boldsymbol{S}^{-}(k) \tag{15}$$

$$\Delta\boldsymbol{U}_{DME}(k) = \begin{bmatrix} \Delta\boldsymbol{U}_{QPSK}(k) \\ \Delta\boldsymbol{U}_{16QAM}(k) \end{bmatrix} = \begin{bmatrix} \boldsymbol{U}_c(k)_{QPSK} \\ \boldsymbol{U}_c(k)_{16QAM} \end{bmatrix} - \boldsymbol{U}_{DME}(k) \tag{16}$$

As shown in Eq. (16), the upper row of the residual ΔU_{DME} is employed to make $\boldsymbol{U}(k)$ approach the circle formed by QPSK symbols and the lower row is employed to make $\boldsymbol{U}(k)$ approach three circles formed by 16QAM symbols. As a result, the dimensionality of the matrix $\boldsymbol{R}$ doubles. The resultant $\boldsymbol{R}_{DME}$ have its diagonals of $\boldsymbol{R}_{QPSK}$ and $\boldsymbol{R}_{16QAM}$, which are both scaled identities. $\boldsymbol{R}_{QPSK}$ and $\boldsymbol{R}_{16QAM}$ should be set initially according to the measurement noise tolerance of QPSK and 16QAM cases. The minimum Euclidean distance between QPSK symbols is larger than that between 16QAM symbols under the same average power. Consequently, the former format has better tolerance against the measurement noise than the latter one. As a result, $\boldsymbol{R}_{QPSK}$ should be larger than $\boldsymbol{R}_{16QAM}$. In the following discussion, the relationship of $\boldsymbol{R}_{QPSK} = 4 \cdot \boldsymbol{R}_{16QAM}$ is used.

#236586 Received 22 Apr 2015; revised 16 Jul 2015; accepted 17 Jul 2015; published 22 Jul 2015

3. Experiments and discussions

3.1 Experimental setup

The performance of the proposed RD-LKF is experimentally investigated in a PDM-QPSK/16QAM system shown in Fig. (2). An optical I/Q modulator is driven by 28 GSymbol/s 2-level electrical signals for QPSK generation and 14 GSymbol/s 4-level electrical signals for 16QAM generation. In the receiver, the electrical signal after coherent detection are sampled by a real-time oscilloscope at 50GSample/s in QPSK and 80GSample/s in 16QAM. The endless polarization rotation was digitally achieved by a polarization rotation matrix $\boldsymbol{J} = [\cos(kwT_s)\ \sin(kwT_s);\ -\sin(kwT_s)\ \cos(kwT_s)]$ in the DSP section before polarization demultiplexing [2, 14]. The w represents the polarization rotation angular frequency. The sampled data was processed offline and RD-LKF, CMA and MMA are employed for polarization tracking comparison. This is followed by an additional single input single output (SISO) CMA filter with {13 taps, the step size of 5e-4} for QPSK and {11 taps, the step size of 1e-6} for 16QAM to further compensate slowly varying channel effects with long memory. In both CMA/MMA and RD-KLF algorithms 2 samples/symbol are adopted. The algorithms all work in the update manner of symbol by symbol [5]. The bit error ratio (BER) or Q-factor are calculated based on 5 independently acquired 56,000 symbols.

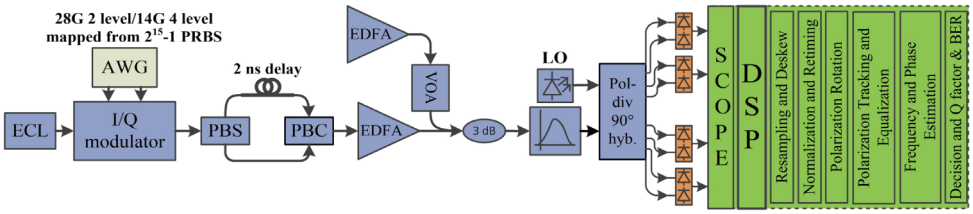

Fig. 2. Experimental setup and digital signal processing modules of a 112 Gb/s PDM-QPSK/PDM-16QAM coherent optical communication system.

3.2 Influence of the tuning parameters on filter performance

In the proposed Kalman filter, the tuning parameters $\boldsymbol{Q}$ and $\boldsymbol{R}$ representing the process noise covariance and measurement noise covariance, should be set properly to optimize the filter performance. It's found from Eqs. (7)-(12) that $\boldsymbol{R}$ and $\boldsymbol{Q}$ can adjust Kalman gain $\boldsymbol{K}$ and consequently change the ratio between the residual and the prediction. With the proper ratio, the filter can achieve the expected balance between tracking speed and estimation accuracy. Based on the analysis presented in Section 2.2, $\boldsymbol{R}$ can be a constant value for a specified modulation format. As an example of illustration, $\{\boldsymbol{R}_{QPSK} = 0.1;\ \boldsymbol{R}_{16QAM} = 0.025\}$ is chosen for $\boldsymbol{R}$ in 16QAM. The left $\boldsymbol{Q}$ parameter should be optimized. In the following the influence of $\boldsymbol{Q}$ value on the filter performance are analyzed and simulated.

The signal distributions of the demultiplexed signals and the estimated $\{a\ b\ c\ d\}$ with three $\boldsymbol{Q}$ parameters of 1e-3, 1e-5 and 1e-7 for Kalman filtering on the same sampled PDM-16QAM data with 3 Mrad/s polarization rotation is shown in Fig. 3. According to Eq. (7), the prediction value is equal to the previous one in order to ensure the continuity and stability of $\{a\ b\ c\ d\}$. In the case of large $\boldsymbol{Q}$ parameter, the prediction proportion decreases, which lead to estimation fluctuation of $\{a\ b\ c\ d\}$. This analysis is consistent with the constellation graph and the estimated curves with $\boldsymbol{Q}$ = 1e-3, shown in Figs. 3(a) and 3(b). However, in case of small $\boldsymbol{Q}$ parameter, the proportion of the prediction values will increase. Meanwhile, the proportion of the residual as a result of time-varying $\{a\ b\ c\ d\}$ decreases. Therefore, the filter can't respond to the variation of $\{a\ b\ c\ d\}$ synchronously, which consequently causes a time delay between the estimated value and the actual value. Obviously, this will degrade polarization tracking performance or even cause tracking failure. As an example, the results under $\boldsymbol{Q}$ = 1e-7 are presented in Fig. 3(e) and 3(f). In agreement with the above analysis, the obvious estimation

#236586 Received 22 Apr 2015; revised 16 Jul 2015; accepted 17 Jul 2015; published 22 Jul 2015

delay is found in Fig. 3(f), in which the blue line presents the estimated a with $\boldsymbol{Q}$ = 1e-7 and the green line presents the estimated a in $\boldsymbol{Q}$ = 1e-5 considered as the actual value. Meanwhile, this delay causes poor polarization tracking performance, as shown in Fig. 3(e). Therefore, the moderate $\boldsymbol{Q}$ should be adopted for an optimal tradeoff between tracking speed and estimation accuracy, as shown in Fig. 3(c) and 3(d) with $\boldsymbol{Q}$ parameter of 1e-5.

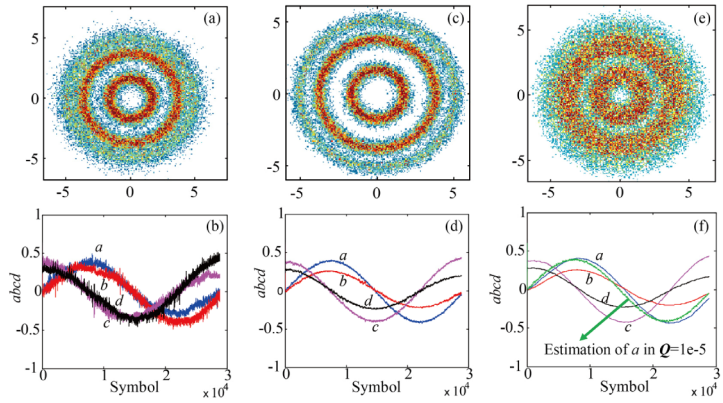

Fig. 3. The constellation graphs after RD-LKF and the estimated {a b c d} with $\boldsymbol{Q}$ = 1e-3 (a, b), $\boldsymbol{Q}$ = 1e-5 (c, d), $\boldsymbol{Q}$ = 1e-7 (e, f).

Furthermore, the BER as a function of optical signal-to-noise ratio (OSNR) under a fast polarization rotation of 3 Mrad/s is also presented with different $\boldsymbol{Q}$ values in the case of 16QAM. In Fig. 4(a), it is clearly found that the algorithm performance can be improved greatly by optimizing $\boldsymbol{Q}$. The optimized $\boldsymbol{Q}$ is around 1e-5 regardless of OSNR at 3 Mrad/s polarization rotation. Figure 4(b) presents the BER as a function of polarization rotation frequency at OSNR of 20.34dB under different $\boldsymbol{Q}$. It can be found that the optimal $\boldsymbol{Q}$ is actually dependent on rotation frequency. At 1 Mrad/s, the optimal $\boldsymbol{Q}$ of 1e-6 can be found. In the next section, $\boldsymbol{Q}$ will be set to be 1e-6 in 16QAM case for RD-LKF scheme to obtain comparable BER performance as MMA scheme at low polarization rotation range, ensuring a fair comparison between their tracking capabilities. Similarly, $\boldsymbol{Q}$ of 1e-5 is chosen in QPSK case in the next section for RD-LKF to obtain comparable performance to CMA scheme at low rotation range.

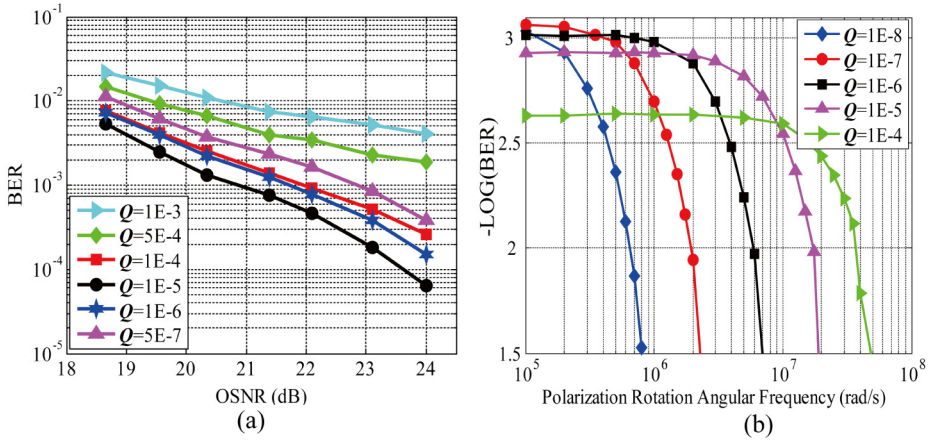

Fig. 4. (a) BER vs. OSNR (dB/0.1nm) under different $\boldsymbol{Q}$ for 3Mrad/s polarization rotation; (b) The BER as a function of polarization rotation frequency under different $\boldsymbol{Q}$.

#236586 Received 22 Apr 2015; revised 16 Jul 2015; accepted 17 Jul 2015; published 22 Jul 2015

3.3 Convergence and tracking performance of RD-LKF

Firstly the convergence performance of RD-LKF is investigated for PDM QPSK and 16QAM signals with OSNR of 15.6dB and 20.34dB, respectively. As confirmed in the above, the tuning parameter $\boldsymbol{Q}$ is critical to optimize the filter performance. Here an elegant strategy of $\boldsymbol{Q}$ setting are employed as follows: during the beginning 20 periods the relatively large value 1e-3 is adopted for increasing the residual proportion and thus speeding up convergence; Later $\boldsymbol{Q}$ is switched to moderate value of 1e-5 and 1e-6 in QPSK and 16QAM, respectively. Figure 5 plots the estimated $\{a\ b\ c\ d\}$ in the first 200 periods with S(0) of $[0.5\ 0.5\ 0.5\ 0.5]^{T}$. We also test the convergence with 20 random S(0) for processing 5 independent sampled signals. It's confirmed that in cases of two modulation formats $\{a\ b\ c\ d\}$ can reach the approximately constant values after around 80 symbols regardless of the initial values.

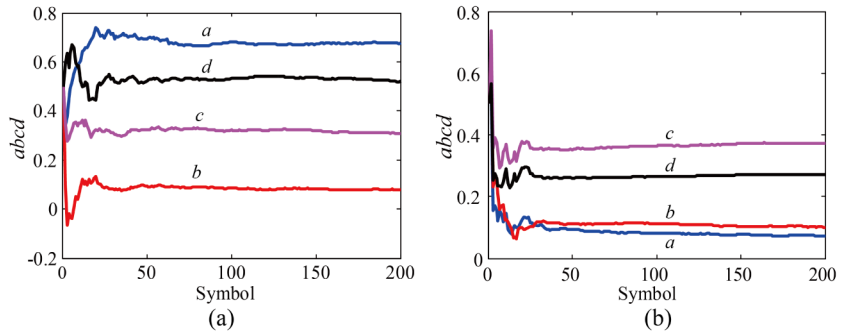

Fig. 5. The estimated parameters *a*, *b*, *c* and *d* for (a) PDM QPSK and (b) PDM 16QAM.

In the following, the tracking performance of RD-LKF against polarization rotation is discussed. The tuning parameter of Q is fixed at 1e-5 and 1e-6 for PDM QPSK and 16QAM for fair comparison with CMA/MMA, respectively. In the case of PDM-QPSK, the Q-factor between RD-LKF and CMA as a function of polarization rotation angular frequency is compared, as shown in Fig. 6(a). The taps, step size u of CMA are set to 3 and 1e-4, respectively. With 0.5dB Q-factor penalty, RD-LKF can track the polarization rotation angular frequency at 38 Mrad/s, which is more than 20 times faster than that of CMA along with around 0.05dB Q-factor degradation in slow rotation regime. The comparison between RD-LKF and MMA is presented in Fig. 6(b). The taps, step size u of MMA is set to 3 and 1e-4, respectively. RD-LKF can track up to 2.5 Mrad/s polarization rotation with 0.5dB Q-factor penalty, which is more than 8 times faster than that of MMA.

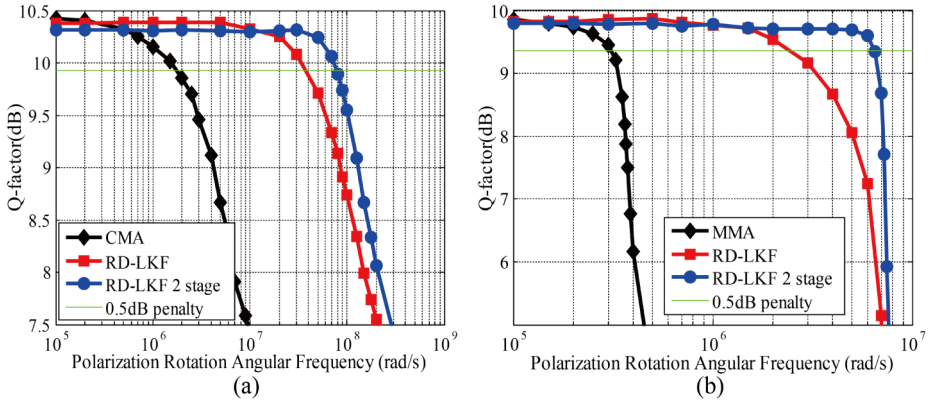

Fig. 6. Q-factor performance versus polarization rotation angular frequency for (a) QPSK and (b) 16QAM.

#236586 Received 22 Apr 2015; revised 16 Jul 2015; accepted 17 Jul 2015; published 22 Jul 2015

Finally it is interesting to point out that cascading two of the same RD-LKF employed above (Fig. 7) can further improve polarizaiton tracking performance, as shown in Fig. 6. This result is due to the fact that the estimation delay of the first stage RD-LKF can be compensated in the following second stage, so that higher polarization roatation angular frequency can be tracked. Meanwhile around 0.05dB Q-factor degradation at slow rotation regime is present for QPSK case along with tracking ability improvement. It can be seen from Fig. 6 that with 0.5dB Q-factor penalty, two stage RD-LKF improves polarization tracking speed by 2 and 2.5 times compared to single stage for QPSK and 16QAM, respectivly.

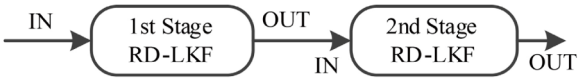

Fig. 7. The scheme of two stage RD-LKF.

4. Conclusions

We have proposed and experimentally demonstrated a RD-LKF scheme to track polarization-state for both PDM QPSK and 16QAM signals. The estimated Jones matrix can reach the approximately constant value after about 80 symbols with the adaptive tuning parameter. The maximal polarization rotation angular frequency it can track are around 40 times of CMA in QPSK format and 20 times of MMA in 16QAM with two stage RD-LKF. The moderate tuning parameters in RD-LKF should be set to obtain a trade-off between tracking speed and estimation accuracy. The cascaded stages of RD-LKF can employed to further improve polarization tracking ability effectively. The scheme is insensitive to carrier phase and the frequency offset and immune to singularity. Therefore, it is suitable to deal with rapidly time-varying polarization-state signals, accurate metrology of PDM signals, and burst-mode coherent receiver that only samples short segments of received data for signal recovery or monitoring.

Acknowledgments

This work is supported by the National Natural Science Foundation of China (contracts no. 61205046, 61435006 and 61377093), Hong Kong Government General Research Fund under project number PolyU 152079/14E and Hong Kong Polytechnic University under project H-ZDA9.

#236586 Received 22 Apr 2015; revised 16 Jul 2015; accepted 17 Jul 2015; published 22 Jul 2015